

## Magnesia grain size effect on *in situ* spinel refractory castables

M.A.L. Braulio<sup>a</sup>, L.R.M. Bittencourt<sup>b</sup>, V.C. Pandolfelli<sup>a,\*</sup>

<sup>a</sup> Federal University of São Carlos, Materials Engineering Department,  
Materials' Microstructural Engineering Group (GEMM), FIRE Associate Laboratory,  
Km 235, Rod. Washington Luís, 13565-905 São Carlos, SP, Brazil

<sup>b</sup> Magnesita S. A., Research and Development Center, 240 Pr. Louis Enschede,  
Contagem, MG, Brazil

Received 19 January 2008; received in revised form 27 April 2008; accepted 9 May 2008

Available online 30 June 2008

### Abstract

Alumina–magnesia castables present an expansive behavior due to *in situ* spinel formation and the reaction is affected by the magnesia source and its grain size. In this study, castables were prepared with different magnesia grain sizes (<45 or <100 μm) and the samples were evaluated by an assisted sintering technique, mechanical strength, creep resistance and microstructural evaluation. The expansion, the resulting phases and properties scaled with the magnesia grain size. The use of coarse MgO grain (<100 μm) led to phases which were predicted by local equilibrium phase diagrams, such as forsterite and monticellite. Due to a completely different microstructure developed for the castable containing large grains, a large number of cracks were generated, worsening the mechanical strength and creep resistance. Magnesia grain size selection is thus a key issue for alumina–magnesia castable design, as it affects the material's performance during service. As the change of a single parameter affected the final castable microstructure and properties, this study is a typical example concerning the complexity of refractory ceramic systems.

© 2008 Elsevier Ltd. All rights reserved.

**Keywords:** Grain size; MgO; Spinel; Refractories; Microstructure

### 1. Introduction

An important aspect to be considered in alumina–magnesia castable design is the magnesia source selection, as it affects various processing steps. Fast flow decay and cracking due to MgO hydration are the main problems observed during placement, setting and drying steps.<sup>1–4</sup> Furthermore, aspects such as MgO grain size, purity and reactivity influence not only magnesia hydration but also spinel formation.

Impurities commonly present in dead-burnt magnesia are silica, lime, iron oxide, alumina and boron oxide. These impurities are combined with MgO, resulting in various calcium silicates and calcium magnesium silicates, among others. According to Landy,<sup>5</sup> the CaO/SiO<sub>2</sub> wt. ratio (C/S) controls the compounds in MgO particles: high CaO contents (ratio >2.8) results in tricalcium silicate (Ca<sub>3</sub>SiO<sub>5</sub>) and free CaO, whereas high SiO<sub>2</sub> amount (ratio <0.93) leads to monticellite (CaMgSiO<sub>4</sub>) and

forsterite (Mg<sub>2</sub>SiO<sub>4</sub>). This ratio also affects the properties at high temperatures. When the SiO<sub>2</sub> content increases (lower CaO/SiO<sub>2</sub> ratio), the initial melting temperature of MgO particles decreases (varying from ~1850 °C for high CaO contents to ~1500 °C for high SiO<sub>2</sub> amounts).<sup>5,6</sup>

The C/S ratio and the MgO purity also affect the *in situ* spinel formation. However, this takes place in an indirect way as increasing the C/S ratio and the magnesia content results in higher brucite formation and, therefore, during sintering, the magnesia chemical activity is enhanced, increasing the spinel formation driving force.<sup>7</sup>

Considering this aspect, the use of coarse MgO grains seems to be a way to control magnesia hydration, as it is a surface-controlled effect. Nevertheless, the magnesia grain size increase affects the *in situ* spinel formation, reducing the spinel content and increasing the overall expansion. Additionally, if some coarse MgO grains do not react, cracks can be developed, due to the thermal expansion mismatch between magnesia and spinel.<sup>7,8</sup>

Alumina–magnesia castables bonded with calcium aluminate cements present an additional expansion component, due to CA<sub>2</sub>

\* Corresponding author.

E-mail address: [vicpando@power.ufscar.br](mailto:vicpando@power.ufscar.br) (V.C. Pandolfelli).

Table 1  
Chemical composition of the selected magnesia source for the whole analyzed batch

Oxide	Typical content (wt%)	Minimum value (wt%)	Maximum value (wt%)
MgO	95.37	95.00	–
CaO	0.43	–	0.60
SiO <sub>2</sub>	1.16	–	1.50
Al <sub>2</sub> O <sub>3</sub>	0.32	–	0.50
Fe <sub>2</sub> O <sub>3</sub>	1.82	–	2.50
MnO	0.91	–	1.00
B <sub>2</sub> O <sub>3</sub>	0.007	–	–

and CA<sub>6</sub> formation.<sup>9–12</sup> Ide et al.<sup>13</sup> studied the magnesia grain size effect on CA<sub>6</sub> formation, suggesting that there is an influence not only on spinel formation, but also on CA<sub>6</sub> development. These authors observed that an increase in the magnesia particle size delays the spinel formation, leading to a greater availability of fine alumina for further CA<sub>6</sub> generation.

Another important phenomenon related to MgO grain size is the spinel formation mechanism. According to Soudier,<sup>7</sup> spinel tends to form mainly by the diffusion of Mg<sup>2+</sup> into alumina grains when fine magnesia is used. On the other hand, in the presence of coarse magnesia, spinel was observed at the border of large magnesia particles.

In this paper, the effect of magnesia grain size on *in situ* spinel formation was investigated by an assisted sintering technique, examination of mechanical strength and microstructural characterization. Different reactions took place for the two magnesia sources selected, which affected the castable behavior at high temperatures. This study is a clear example regarding the complexity of ceramic systems, as the change of only one variable had a significant impact on the castable microstructure and, consequently, its final properties.

## 2. Experimental procedure

Two different magnesia grain sizes were analyzed: <45 and <100 μm. Both of them were dead-burnt MgO, containing 95 wt% MgO and 0.37 C/S ratio (Magnesita S. A., Brazil). Their chemical composition is presented in Table 1 and was measured by the X-ray fluorescence (XRF) method.

Vibratable alumina–magnesia castables were designed using a  $q = 0.26$  Alfred packing model. Their matrix comprises 6 wt%

Table 2  
XRD quantitative analyses of alumina–magnesia castables containing different MgO grain sizes (<45 and <100 μm), sintered for 5 h at different temperatures

	Phases					
	Magnesia		Spinel		CA <sub>6</sub>	
	<45 μm	<100 μm	<45 μm	<100 μm	<45 μm	<100 μm
1150 °C	3	6	10	0	–	–
1300 °C	1	6	16	4	–	–
1500 °C	0	2	21	16	14	16

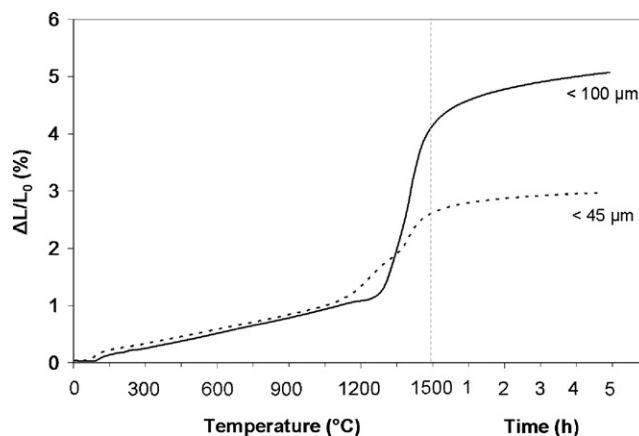


Fig. 1. Expansion behavior of alumina–magnesia castables containing different MgO grain sizes (<45 and <100 μm).

of dead-burnt magnesia (<45 or <100 μm), 7 wt% of reactive alumina (CL370, USA, Almatiss), 6 wt% of calcium aluminate cement (Secar71, Kerneos, France), 1 wt% of microsilica (971U, Elkem) and 15 wt% of fine tabular alumina ( $d \leq 200$  μm, Almatiss, Germany) in order to attain 21 wt% of stoichiometric spinel. Coarse tabular aluminas with different grain sizes were used as aggregates ( $d \leq 6$  mm, Almatiss, Germany).

The water content for suitable shaping was 3.9 wt% for the castable containing the finest MgO and 4.1 wt% for the coarsest one. This small difference can be attributed to the grain size distribution of these magnesium oxides, leading to different particle packing. The dispersion was ensured by adding 0.2 wt% of a polycarboxylate-based dispersant (Bayer, Germany).

The expansive behavior was evaluated by an assisted sintering technique, which was performed on a refractoriness-under-load unit (Model RUL 421E, Netzsch, Germany). Cylindrical samples were prepared according to the 51053 DIN standard, cured at 50 °C and dried at 110 °C for 1 day, followed by pre-firing at 600 °C for 5 h before testing. Samples were heated to 1500 °C at 3 °C/min and kept at this temperature for 5 h. The compression load applied was 0.02 MPa. This test was selected because dilatometric experiments performed only on a castable's matrix are not representative, as shown in a previous study by Braulio

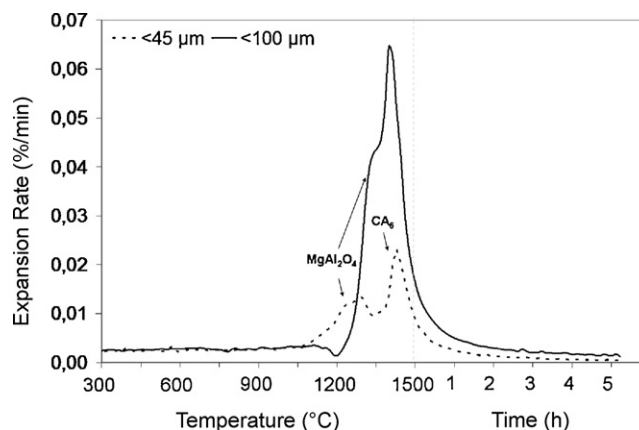


Fig. 2. Expansion rate of alumina–magnesia castables containing different MgO grain sizes (<45 and <100 μm).

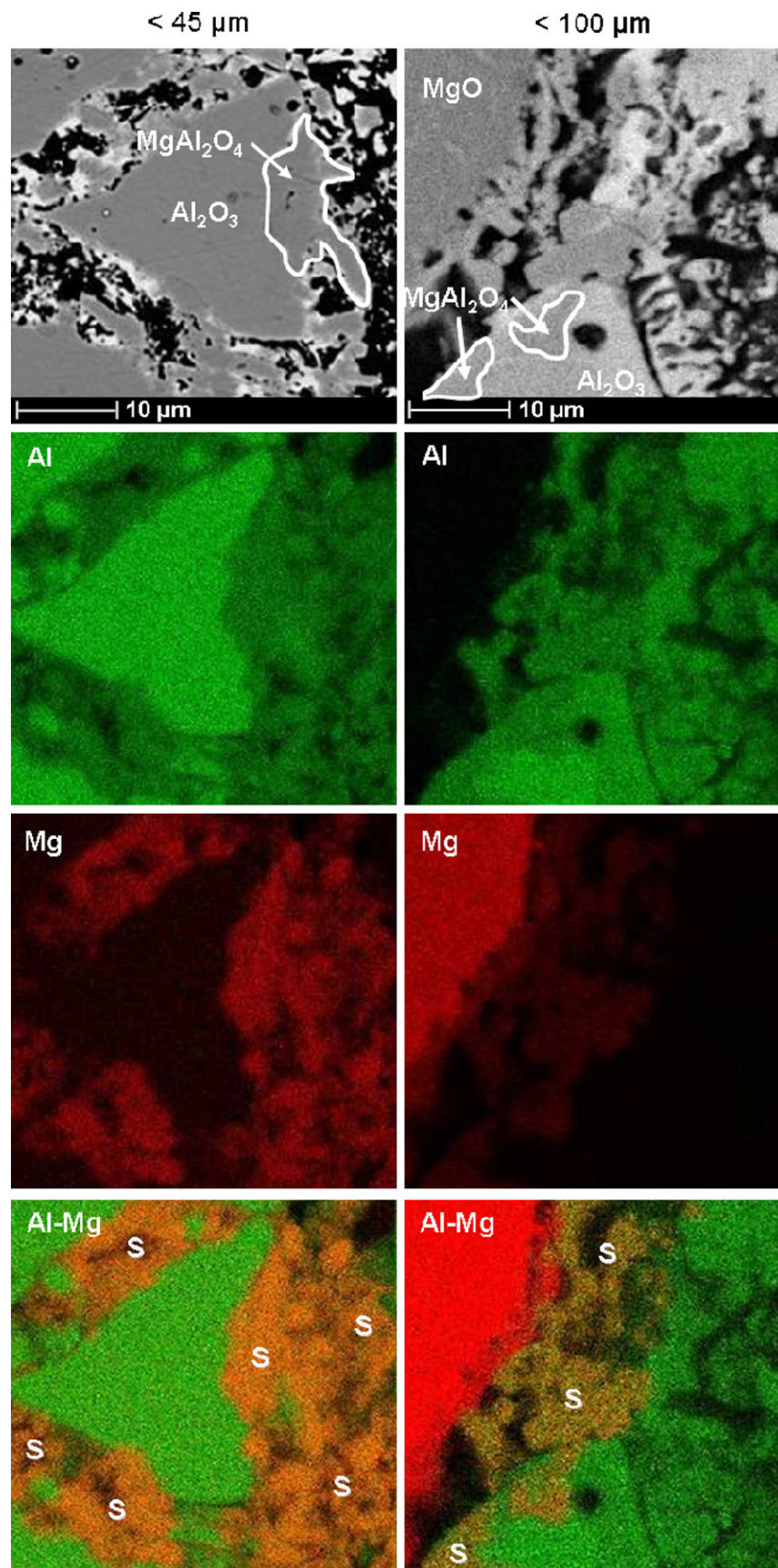


Fig. 3.  $Mg^{2+}$  diffusion after firing at  $1300\text{ }^{\circ}\text{C}$  for alumina–magnesia castables containing different MgO grain sizes ( $<45$  and  $<100\text{ }\mu\text{m}$ ), indicating a higher spinel (S) content for the finer MgO than of the coarser one. The spinel formation template mechanism is observed by the magnesia diffusion into alumina grains.

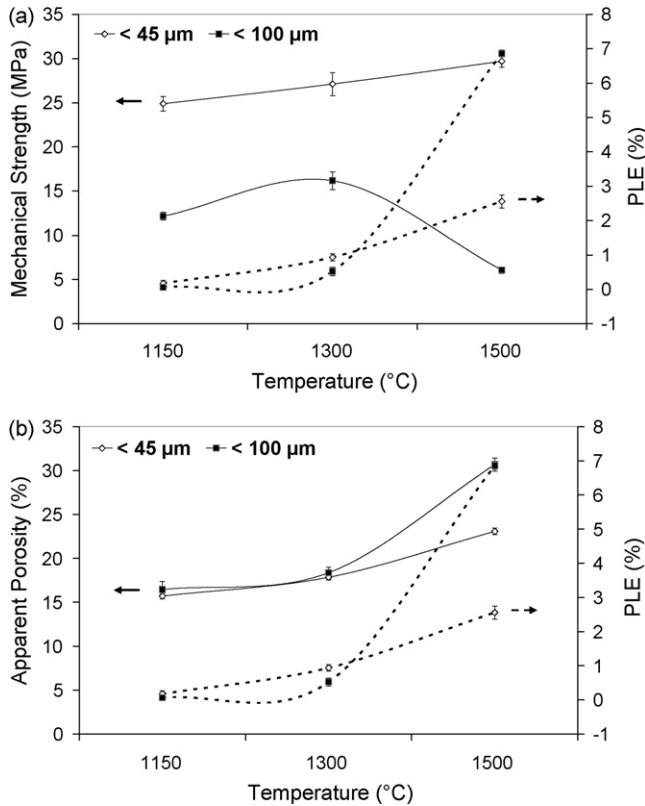


Fig. 4. (a) Mechanical strength versus permanent linear expansion (PLE) and (b) apparent porosity  $\times$  PLE of alumina–magnesia castables containing different MgO grain sizes (<45 and <100  $\mu\text{m}$ ).

et al.,<sup>10</sup> which indicated the effect of a castable's aggregates on the thermal expansion behavior of refractory castables.

Creep measurements were also carried out in the same refractoriness-under-load equipment. Cylindrical samples as described above were previously pre-fired at 1550 °C for 24 h and then analyzed at 1450 °C for 24 h under a constant compression load of 0.2 MPa.

For the mechanical tests and permanent linear expansion (PLE) 25 mm  $\times$  25 mm  $\times$  150 mm bars were prepared. After curing (50 °C, 1 day), drying (110 °C, 1 day) and calcining

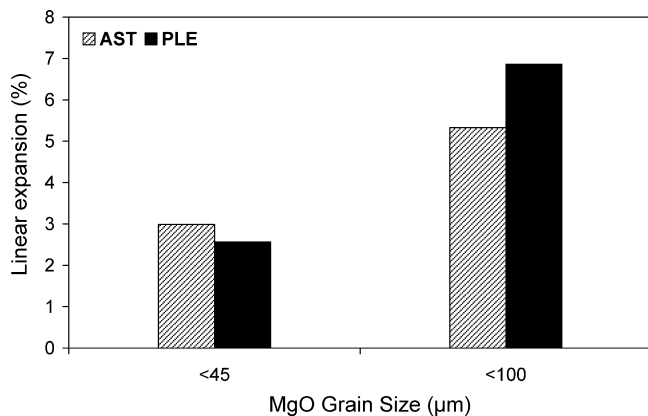


Fig. 5. Linear expansion of alumina–magnesia castables containing different MgO grain sizes (<45 and <100  $\mu\text{m}$ ), after the assisted sintering test (AST) and PLE evaluation.

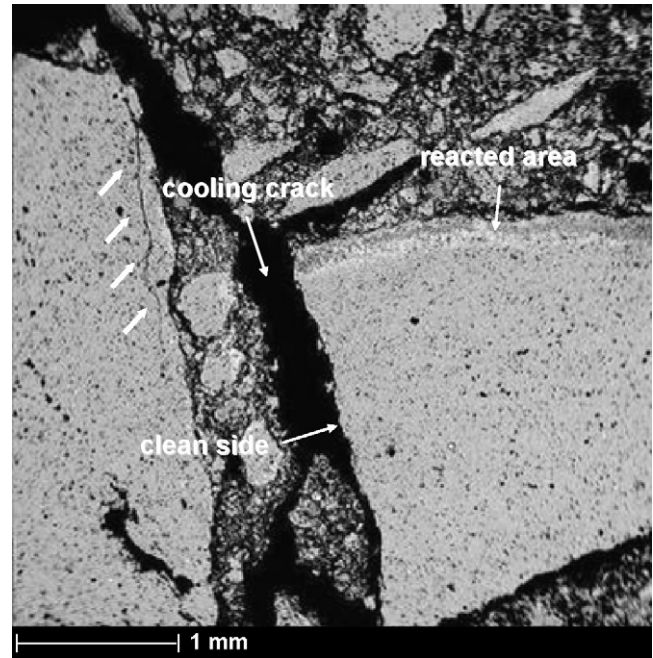


Fig. 6. Cooling crack in the alumina–magnesia castable containing coarse MgO, after firing at 1500 °C.

(600 °C, 5 h), the samples were fired at a heating rate of 1 °C/min at 1150, 1300 and 1500 °C (dwell time 5 h). The modulus of rupture was obtained by the 3-point bending test according to ASTM C133-94 (Standard Test Methods for Cold Crushing Strength and Modulus of Rupture of Refractories) using MTS equipment (MTS Systems, Model 810, USA). The permanent linear expansion was measured by the percentage difference between the final and the initial bar length. Additionally, the apparent porosity of these castables was attained by the usual Archimedes technique.

Phase analyses were performed by X-ray diffraction quantitative test, using software based on the Rietveld method<sup>14</sup> (TOPAS, Bruker, Germany). Scanning electron microscopy and EDS analysis were carried out in order to locate the phases and their distribution in the castable compositions. The XRD and SEM samples were analyzed after firing the castables for 5 h at three different temperatures: 1150, 1300 and 1500 °C, to attain a correlation between expansion and phase evolution.

Furthermore, thermodynamic simulations were also conducted in order to calculate the Gibbs free energy of the reactions at different temperatures (FactSage, Thermfact and GTT-Technologies, Universidade Federal de São Carlos, FAI).

### 3. Results and discussion

#### 3.1. MgO grain size influence on alumina–magnesia castable expansion

Increasing the magnesia grain size resulted in a high thermal expansion, as presented in Fig. 1 and could be related to: (1) the formation of large pores during spinel formation, due to  $\text{Mg}^{2+}$  diffusion and (2) the difference in the  $\text{CA}_6$  formation content for the two MgO grain sizes. The first aspect could be explained

according to Kiyota<sup>15</sup> and Nakagawa,<sup>16,17</sup> who stated that the one-way diffusion of magnesia into alumina grains during *in situ* spinel formation leads to a large permanent expansion in an alumina–magnesia castable, as  $Mg^{2+}$  diffusion is faster than  $Al^{3+}$ .

The derivative expansion curves highlight the effect of coarse magnesia grains during spinel formation, leading to a higher spinel expansion peak rate (Fig. 2). According to a previous publication,<sup>9</sup> the first peak detected in these curves is related to *in situ* spinel formation, whereas the second refers to *in situ* CA<sub>6</sub> formation, as the calcium aluminate cement content in these compositions is high (6 wt%). In the fine MgO sample, two peaks can be detected concerning spinel formation. Díaz et al.<sup>18</sup> had already analyzed a composition where this reaction occurred at different temperatures, due to the broad particles size distribution of MgO grain sizes. Therefore, the two peaks observed can be a consequence of spinel formation by the consumption of fine and coarse MgO grains in the dead-burnt MgO (<45 μm).

Additionally, there is a delay in the *in situ* spinel formation for the coarse MgO grain as the main expansion started at ~1000 °C for the castable containing the <45 μm MgO and at ~1200 °C

for the composition containing the <100 μm one. The different reaction kinetics are represented in Fig. 3 by the largest spinel formation observed for the fine magnesia source, after firing the castables at 1300 °C, as the higher surface area of finer MgO led to its dissolution at lower temperatures, speeding up its diffusion. One important aspect in these SEM micrographs is the spinel template formation mechanism,<sup>19</sup> which indicates that spinel commonly assumes the same morphology as alumina (for MgO <45 μm, spinel was detected in the right side of the alumina grain). Nevertheless, for the coarse MgO source, spinel is also detected at the border of MgO grain, due to its lower diffusion ability. These results are in tune with those stated by Soudier.<sup>7</sup>

As a consequence of its higher expansion, the sample containing the coarse MgO grain showed reduced mechanical strength (Fig. 4a) and an increase in the apparent porosity (Fig. 4b) from 1300 to 1500 °C, which is the temperature range where spinel and CA<sub>6</sub> are developed. A great number of surface cracks were observed in this composition, after firing at 1500 °C. In order to understand whether these cracks were formed during heating (due to spinel and CA<sub>6</sub> formation) or cooling (associated with the different thermal expansion coefficient among the phases),

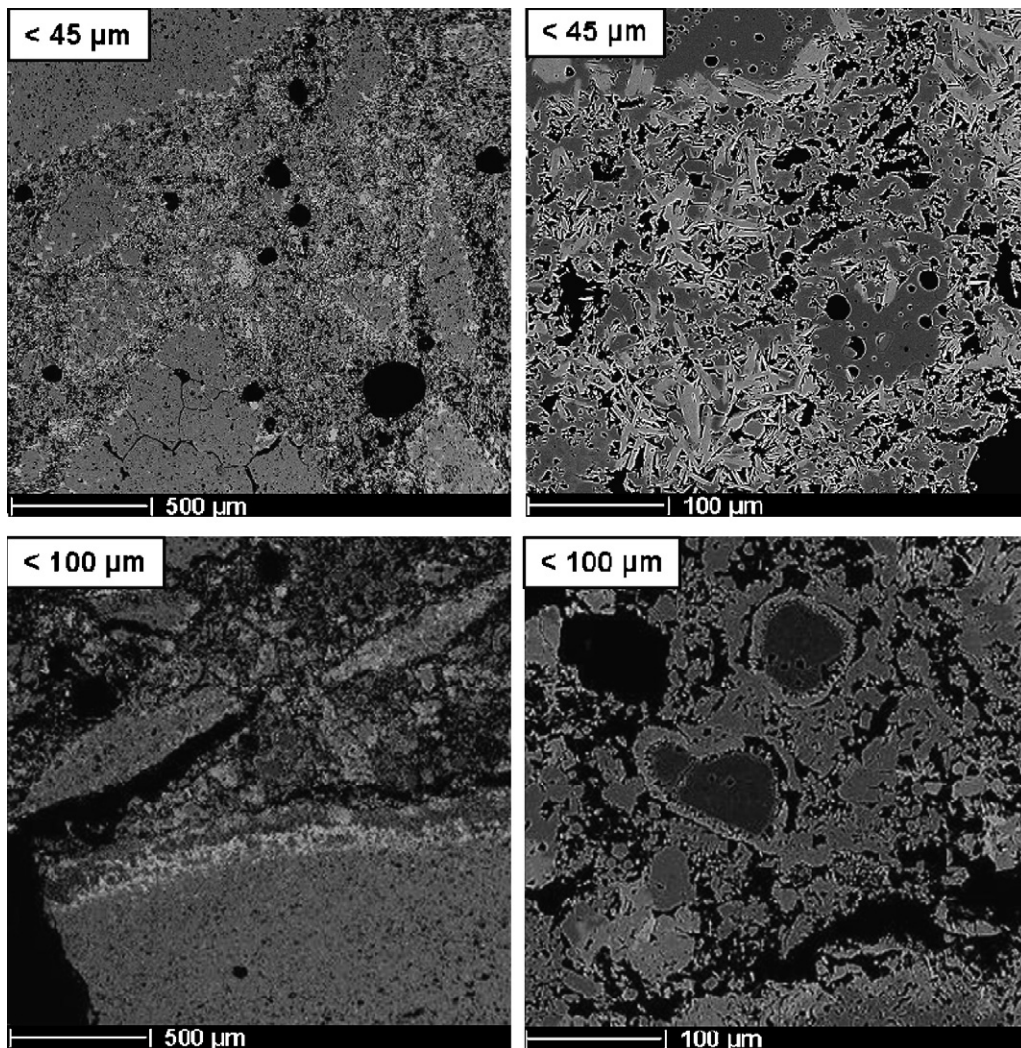


Fig. 7. Microstructures of alumina–magnesia castables containing different MgO grain sizes (<45 and <100 μm), after firing at 1500 °C for 5 h.

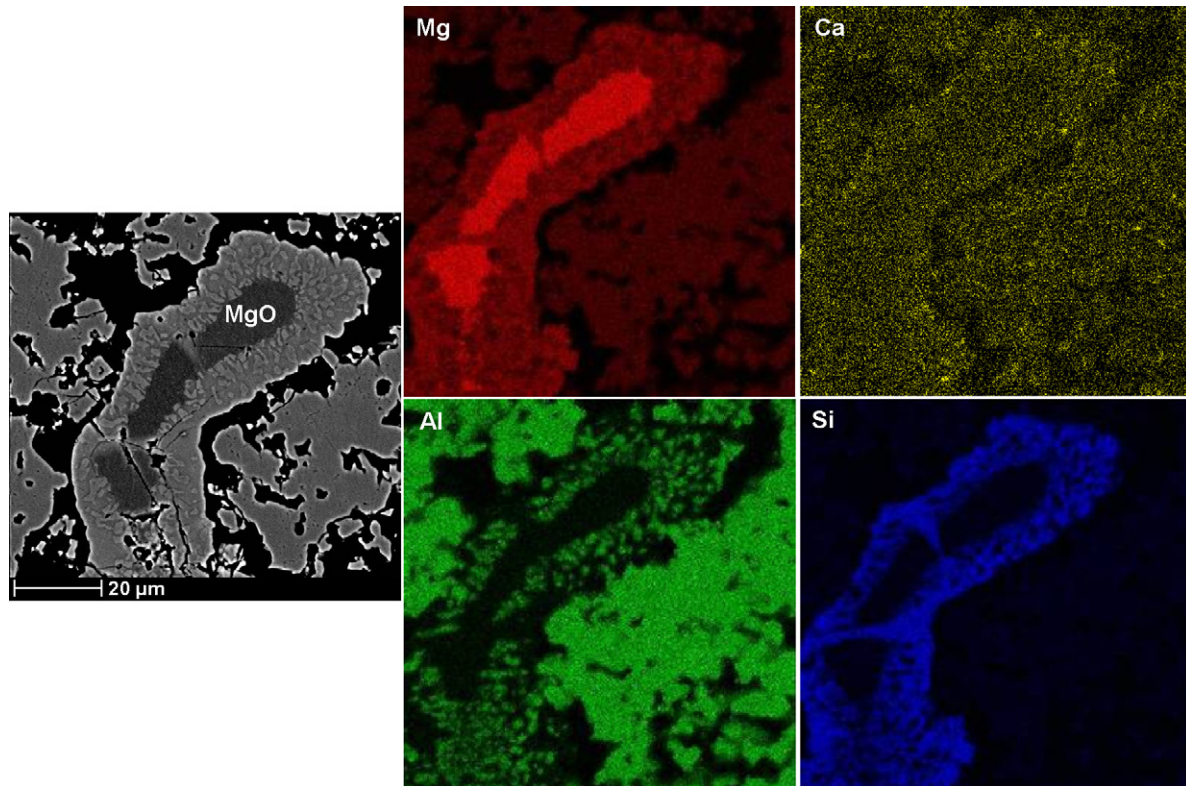


Fig. 8. Forsterite ( $\text{Mg} + \text{Si}, \text{Mg}_2\text{SiO}_4$ ), monticellite ( $\text{Ca} + \text{Mg} + \text{Si}, \text{CaMgSiO}_4$ ) and spinel ( $\text{Mg} + \text{Al}, \text{MgAl}_2\text{O}_4$ ) layer (represented by the ions combination distribution, obtained by quantitative EDS analyses) at the border of a magnesia grain, for the alumina–magnesia castable containing  $\text{MgO} < 100 \mu\text{m}$ , after firing at  $1500^\circ\text{C}$  for 5 h.

the overall expansion after the assisted sintering test (AST) was compared with the permanent linear expansion (PLE) after firing at  $1500^\circ\text{C}$  and are presented in Fig. 5. The castable containing the fine  $\text{MgO}$  source indicated AST expansion close to the PLE one, which suggests that no further cracks were developed during cooling. Conversely, the coarse magnesia source castable resulted in  $\text{AST expansion} < \text{PLE}$ , indicating that cracks were most likely formed during cooling.

This result is attested by Fig. 6, where a typical cooling crack is detected for the  $<100 \mu\text{m}$   $\text{MgO}$  castable, after firing at  $1500^\circ\text{C}$ . The crack was assumed to be formed on cooling because the tabular alumina grain at the right side of the figure showed reaction at the upper part (leading to  $\text{CA}_6$  formation), but its left side was clean, indicating that the crack was formed due to the thermal expansion coefficient mismatch between alumina, spinel and the remnant  $\text{MgO}$ . Additionally, the arrows on the left tabular alumina highlighted that this grain was also at the crack splitting imminence.

In order to better understand these results, XRD quantitative analyses were carried out for samples fired at  $1150$ ;  $1300$  and  $1500^\circ\text{C}$  (Table 2). Three special features can be identified in this table: (1) the faster spinel formation for the fine  $\text{MgO}$  source composition; (2) the presence of unreacted  $\text{MgO}$  for the coarse magnesia source castable after firing at  $1500^\circ\text{C}$  and (3) the higher amount of  $\text{CA}_6$  for the sample containing the large  $\text{MgO}$  grain size. The first aspect is associated with the slightly high permanent linear expansion observed after firing at  $1150$  and  $1300^\circ\text{C}$  for the castable containing fine  $\text{MgO}$

(Fig. 4), as a considerable amount of spinel was produced. The second and third aspects were related to the higher permanent linear expansion observed after firing at  $1500^\circ\text{C}$  for the coarse  $\text{MgO}$  source. Additionally, the higher  $\text{CA}_6$  generation for the coarse  $\text{MgO}$  castable is consistent with a previous study by Ide et al.<sup>13</sup>.

### 3.2. The refractory castables' complexity

Changing the magnesia grain size of alumina–magnesia castables completely affected the phase development at high temperatures and their distribution throughout the castable. Fig. 7 shows their different microstructures, after firing at  $1500^\circ\text{C}$ . The castable containing the fine  $\text{MgO}$  presented alumina, spinel (77 wt%  $\text{Al}_2\text{O}_3$ –23 wt%  $\text{MgO}$ ) and  $\text{CA}_6$ , which are the traditional expected phases for this sort of material. Nevertheless, the composition containing the coarse  $\text{MgO}$  comprised alumina, magnesia,  $\text{CA}_6$ , spinel (70 wt%  $\text{Al}_2\text{O}_3$ –30 wt%  $\text{MgO}$ ), forsterite ( $\text{Mg}_2\text{SiO}_4$ ) and most likely monticellite ( $\text{CaMgSiO}_4$ ). One important aspect in the coarse  $\text{MgO}$  castable microstructure is the large pores and cracks observed, which led to the higher expansion.

In some partially reacted magnesia grains for the  $<100 \mu\text{m}$  alumina–magnesia castable fired at  $1500^\circ\text{C}$ , forsterite, spinel and monticellite were observed at their border by quantitative EDS analyses, which is a particular feature of this composition (Fig. 8). According to Myhre and co-workers,<sup>20,21</sup> the forsterite formation is commonly carried out at above roughly

1000 °C and is accompanied by shrinkage. Cunha-Duncan and Bradt<sup>22</sup> also analyzed this aspect and concluded that, from a thermodynamics standpoint, the formation of forsterite is more favorable than the spinel one. In order to check this statement, thermodynamics simulations were performed and the free energy was calculated for these three reactions at different temperatures (Fig. 9). As the free Gibbs energy is more negative for forsterite and monticellite, they are thermodynamically more favorable than spinel. Consequently, considering a local equilibrium for the coarse MgO and that remnant magnesia was present at 1500 °C, forsterite and monticellite were formed.

It is important to consider the C/S ratio of this magnesia source and its slower reaction kinetics in order to better understand this forsterite and monticellite formation only for the coarse MgO castable. The C/S ratio of the MgO selected is 0.37, which leads, according to Landy,<sup>5</sup> to monticellite (CaMgSiO<sub>4</sub>) and forsterite (Mg<sub>2</sub>SiO<sub>4</sub>) as accessory minerals. Conversely for the fine MgO grain size where magnesia is easily dissolved and ready to react with alumina producing spinel, in the coarse magnesia there is less dissolution, retarding spinel formation and providing time for magnesia–silica–alumina–calcia interaction, leading to spinel, forsterite and monticellite formation. The layer formed by these phases inhibits the inner part of the MgO grain from reacting and as a result remnant MgO is still present after firing at 1500 °C for 5 h.

The different phases observed for the coarse MgO castable points out the limitation of thermodynamic equilibria calculations, as discussed previously by Lee et al.<sup>23</sup>. According to these authors, this sort of calculations is suitable for nanometer scale and intimately mixed powders, where the equilibrium is rapidly attained. Nevertheless, for coarser grains (MgO < 100 μm), the local equilibrium must be considered, which in the present research favored the forsterite and monticellite formation.

This composition special feature is an example concerning the refractory castable's complexity, as varying the particle size of only one raw material strongly affected the microstructure after sintering, clearly changing the castable properties, as the creep resistance.

The creep behavior of refractory castables especially depends on three microstructural issues: (i) the apparent porosity, (ii)

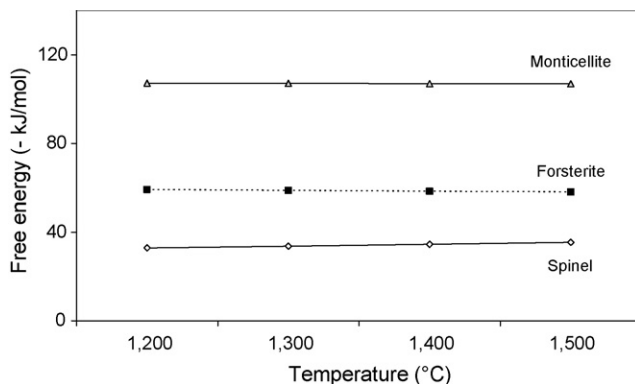


Fig. 9. Free energy for forsterite, spinel and monticellite formation, at different temperatures (FactSage, Universidade Federal de São Carlos, FAI).

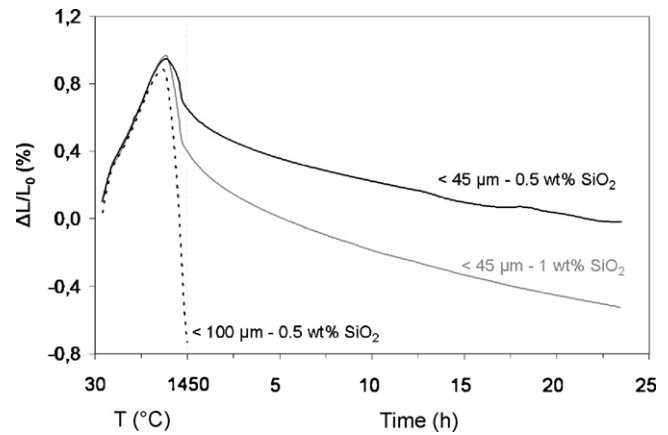


Fig. 10. Creep resistance of alumina–magnesia castables containing different MgO grain sizes (<45 and <100 μm) and microsilica content (0.5 and 1 wt%).

the amount, composition and distribution of glassy phases and (iii) the size, morphology and distribution of the crystalline phases. The addition of coarse grains should favor a greater creep resistance. Nevertheless, as a great number of large cracks were developed and monticellite was generated it was not even possible to obtain the creep curve for this magnesia source when the composition contained 1 wt% of SiO<sub>2</sub>. Even with the microsilica reduction (from 1 to 0.5 wt%), which resulted in a smaller apparent porosity and expansion, the creep resistance was worse than that observed in the sample containing the fine magnesia source, either with 1 or 0.5 wt% of silica, as Fig. 10 indicates.

#### 4. Conclusions

Selecting the magnesia grain size is a key issue to alumina–magnesia design, as it affects the castable microstructure after firing. The effect of these different developed phases can be briefly summarized as follows:

- A high spinel and CA<sub>6</sub> expansion can result in cracks, increasing the castable porosity and worsening the mechanical behavior.
- The creep resistance is better for the sample containing the fine MgO source, as fewer cracks develop and because monticellite is not detected. Nevertheless, compositions presenting coarse MgO grains might present better thermal shock damage resistance, due to the great number of pores, to the higher needle-like CA<sub>6</sub> formation and to the presence of MgO and Mg<sub>2</sub>SiO<sub>4</sub>, as these two phases have higher thermal expansion coefficients than alumina and spinel, resulting in a thermal expansion mismatch.<sup>24,25</sup>
- Because the spinel particle size is larger and its content is lower, using the coarser magnesia source, large pores and cracks are created, which might spoil the slag infiltration and the chemical corrosion resistance of such castables.
- As alumina–magnesia castables are commonly used in steel ladles, they are fired under mechanical constraining. This could improve the thermo-mechanical behavior, due to the development of a toughening mechanism. Further studies will

be carried out in order to understand the development of these phases under constraint, which will most likely affect the properties mentioned above.

## Acknowledgments

The authors are grateful to the Federation for International Refractory and Education (FIRE), Magnesita S. A. (Brazil) and the Brazilian Research Funding FAPESP for supporting this work. Additionally, the authors are thankful to D.H. Milanez and E.Y. Sako (GEMM) for the castable processing step, to Prof. J. Poirier and A. Genty (Polytech' Orléans, France) for the support in the SEM and XRD analyses and to Prof. M. Rigaud (École Polytechnique Montréal, Canada) for his comments.

## References

- Odegard, C., Myhre, B., Zhou, N. and Zhang, S., Flow and properties of MgO based castables. In *XXXII ALAFAR Congress Proceedings*, 2004, p. 11.
- Bier, T. A., Parr, C., Revais, C., Vialle, M. and Fryda, H., Chemical interaction of MgO in spinel forming castables. In *XXVII ALAFAR Congress Proceedings*, 1998, p. 8.
- Razouk, R. I. and Mikhail, R. S., The hydration of magnesium oxide from vapor phase. *Journal of Physical Chemistry*, 1958, **62**, 920–925.
- Kitamura, A., Onizuka, K. and Tanaka, K., Hydration characteristics of magnesia. *Taikabutsu Overseas*, 1995, **16**(3), 3–11.
- Landy, R. A., *Magnesia Refractories. Refractories Handbook*. Marcel Dekker Inc., 2004, pp. 109–149.
- Aksel, C., Kasap, F. and Sesver, A., Investigation of parameters affecting grain growth of sintered magnesite refractories. *Ceramics International*, 2005, **31**, 121–127.
- Soudier, J., Understanding and optimisation of MgO hydration resistance and spinel formation mechanisms for increasing performances of DVM used in crucible induction furnaces melting steel. In *UNITECR'05 Proceedings*, 2005, pp. 679–683.
- Zhang, S. and Lee, W. E., *Spinel-containing Refractories. Refractories Handbook*. Marcel Dekker Inc., 2004, pp. 215–258.
- Braulio, M. A. L., Milanez, D. H., Sako, E. Y., Bittencourt, L. R. M. and Pandolfelli, V. C., Expansion behavior of cement bonded alumina–magnesia refractory castables. *American Ceramic Society Bulletin*, 2007, **86**(12), 9201–9206.
- Braulio, M. A. L., Milanez, D. H., Sako, E. Y., Bittencourt, L. R. M. and Pandolfelli, V. C., Are refractory aggregates inert? *American Ceramic Society Bulletin*, 2007, **87**(3), 27–31.
- Braulio, M. A. L., Bittencourt, L. R. M., Poirier, J. and Pandolfelli, V. C., Microsilica effects on cement bonded alumina–magnesia refractory castables. *Journal of the Technical Association of Refractories, Japan*, in press.
- Auvray, J. M., Gault, C. and Huger, M., Evolution of elastic properties and microstructural changes versus temperature in bonding phases of alumina and alumina–magnesia refractory castables. *Journal of the European Ceramic Society*, 2007, **27**, 3489–3496.
- Ide, K., Suzuki, T., Asano, K., Nishi, T., Isobe, T. and Ichikawa, H., Expansion behavior of alumina–magnesia castables. *Journal of the Technical Association of Refractories*, 2005, **25**(3), 202–208.
- Rietveld, H. M., A profile refinement method for nuclear and magnetic structures. *Journal of Applied Crystallography*, 1969, **2**, 65–71.
- Kiyota, Y., Reduction of permanent linear change of Al<sub>2</sub>O<sub>3</sub>–MgO castable. In *UNITECR'07 Proceedings*, 2007, pp. 546–549.
- Nakagawa, Z., Expansion behavior of powder compacts during spinel formation. *Mass and Charge Transport in Ceramics*, 1996, 283–294.
- Nakagawa, Z., Enomoto, N., Yi, I. and Asano, K., Effect of corundum/periclase sizes on expansion behavior during synthesis of spinel. In *UNITECR'95 Proceedings*, 1995, pp. 379–386.
- Díaz, L. A., Torrecillas, R., De Aza, A. H., Pena, P. and De Aza, S., Alumina-rich refractory concretes with added spinel, periclase and dolomite: a comparative study of their microstructural evolution with temperature. *Journal of the European Ceramic Society*, 2005, **25**, 1499–1506.
- Jayaseelan, D. D., Zhang, S., Hashimoto, S. and Lee, W. E., Template formation of magnesium aluminate (MgAl<sub>2</sub>O<sub>4</sub>) spinel microplatelets in molten salt. *Journal of the European Ceramic Society*, 2007, **27**, 4745–4749.
- Myhre, B., Sandberg, B. and Hundere, A. M., Castables with MgO–SiO<sub>2</sub>–Al<sub>2</sub>O<sub>3</sub> as bond phase. In *XXVI ALAFAR Congress Proceedings*, 1997, p. 10.
- Odegard, C., Feldborg, H. and Myhre, B., Magnesia–silicate–hydrate bonded MgO castables. In *UNITECR'01 Proceedings*, 2001, p. 4.
- Cunha-Duncan, F. N. and Bradt, R. C., Synthesis of magnesium aluminate spinels from bauxites and magnesias. *Journal of American Ceramic Society*, 2002, **85**(12), 2995–3003.
- Lee, W. E., Argent, B. B. and Zhang, S., Complex phase equilibria in refractories design and use. *Journal of American Ceramic Society*, 2002, **85**(12), 2911–2918.
- Carniglia, S. C. and Barna, G. L., *Handbook of Industrial Refractories Technology*. Noyes Publications, 1992, pp. 182–183.
- Rigaud, M., Palco, S. and Wang, N., Spinel formation in the MgO–MgAl<sub>2</sub>O<sub>4</sub> system relevant to basic castables. In *UNITECR'95 Proceedings*, 1995, pp. 387–394.